Journal of Solid State Chemistry **142,** 174–179 (1999)
Article ID jssc.1998.8020, available online at http://www.idealibrary.com on IDEAL®

Antiphase Modulated Structure of $Fe_2O_3(ZnO)_{15}$ Studied by High-Resolution Electron Microscopy

Chunfei Li,* Yoshio Bando,* Masaki Nakamura,* and Noboru Kimizuka†

*National Institute for Research in Inorganic Materials, 1-Namiki, Tsukuba, Ibaraki 305, Japan; and †Universidad de Sonora, CIPM, Hermosillo, Sonora, C.P. 83000, Mexico

Received April 27, 1998; in revised form August 31, 1998; accepted September 9, 1998

As one of our systematic studies of the modulated structures of a series of new homologous compounds $RMO_3(ZnO)_m$ (R = Sc, In, Y, and La; M = In, Fe Ga, and Al; m = integer), this paper reports the modulated structure of $Fe_2O_3(ZnO)_{15}$ (R = Fe; M = Fe) studied by high-resolution electron microscopy. It is found that the main and satellite spots in the diffraction patterns can be indexed as $h\mathbf{a}^*+k\mathbf{b}^*+l\mathbf{c}^*+m\mathbf{q}$ by considering a monoclinic unit cell of $a = 0.57$ nm, $b = 0.33$ nm, $c = 4.5$ nm, and $\beta = 92^\circ$ and a modulation wave vector of $\mathbf{q} = \mathbf{b}^*/34.8+\mathbf{c}^*/2$. The possible space groups for the basic structure are $C2$, Cm, and $C2/m$, and the possible four-dimensional superspace groups for the modulated structure are C_1^{C2}, $C_{\bar{1}}^{Cm}$, and $C_{1\bar{1}}^{C2/m}$. The crystal structure of $Fe_2O_3(ZnO)_{15}$ consists of Fe–O layers interleaved with 16 Fe/Zn–O layers. In the high-resolution image, the modulated structure appeared as zigzag-shaped contrasts among the Fe/Zn–O layers, where Fe is in high concentration. Compared with those of $InMO_3(ZnO)_m$ (R = In; M = In, Fe and Ga) reported in our earlier paper, the special features of the present modulated structure are the half-periodicity relative shift of the neighboring zigzag-shaped contrasts and the appearance of modulation within the Fe–O layers. © 1999 Academic Press

1. INTRODUCTION

The structures of a series of new homologous compounds $RMO_3(ZnO)_m$ (R = Sc, In, Y, and La; M = In, Fe, Ga, and Al; m = integer) have been studied by X-ray diffraction analysis (1–6). It was suggested that $RMO_3(ZnO)_m$ is a layered structure, consisting of RO_2^- (R–O) and $MZn_mO_{m+1}^+$ (M/Zn–O) layers stacked alternately. The R ions in the R–O layer occupy the octahedral sites of close-packed O ions, while M and Zn in M/Zn–O layers occupy the tetragonal or trigonal-bipyramidal sites. A schematic drawing of a block built up of one R–O and $m + 1$ M/Zn–O layers is shown in Fig. 1, where m is taken as 6. The space groups were assigned as $R\bar{3}m$ for compounds with odd m and $P6_3/mmc$ for those with even m. The distribution of M and Zn in the M/Zn–O layers was considered to be random (7, 8).

Among these compounds, the structures of $InMO_3(ZnO)_m$ (R = In; M = In, Fe, and Ga) have been studied by high-resolution electron microscopy (6, 9–13). The formation of a modulated structure was revealed (9–13). In the high-resolution image, the modulated structure appeared as zigzag-shaped contrasts among the M/Zn–O layers, where the ordering of M ions was verified by composition analysis using an analytical electron microscope. The symmetry of the modulated structure was successfully analyzed by the four-dimensional superspace group approach. The main and satellite spots in the electron diffraction pattern were indexed as $h\mathbf{a}^* + k\mathbf{b}^* + l\mathbf{c}^* + m\mathbf{q}$, where $\mathbf{a}^*$, $\mathbf{b}^*$, and $\mathbf{c}^*$ are the reciprocal lattice base vectors for the basic structure and $\mathbf{q} = \mathbf{b}^*/s$ is the modulation wave vector. $\mathbf{a}$, $\mathbf{b}$, and $\mathbf{c}$ form monoclinic ($\mathbf{b}$ is the unique axis) or orthorhombic unit cells depending on m = odd or even numbers, respectively. It should be pointed out that although the above symmetry analysis applies to the entire $InMO_3(ZnO)_m$ system, the detailed features of the modulated structure depend on the kind of ion M. For example, the value of s in $InFeO_3(ZnO)_m$ (M = Fe) is about twice that of $In_2O_3(ZnO)_m$ (M = In). With respect to R ions, since no modulated structure in the In–O layer was observed in the $InMO_3(ZnO)_m$ system and there are no reports about the modulated structure in other $RMO_3(ZnO)_m$ systems where R is different from In, the effect of the R ion on the formation of the modulated structure remains unknown.

To clarify this problem, the modulated structure of $Fe_2O_3(ZnO)_{15}$ (R = Fe; M = Fe) is studied by high-resolution electron microscopy and the results are compared with those of $InFeO_3(ZnO)_m$ (R = In; M = Fe). Three special features of the modulated structure of $Fe_2O_3(ZnO)_{15}$ which have not been observed in the previous experiments (10–13) are revealed: the existence of the rational part $\mathbf{c}^*/2$ in the modulation wave vector $\mathbf{q}$, the half-periodicity relative shift of the neighboring zigzag-shaped modulated structure contrasts in the high-resolution image, and the formation of a modulated structure in the Fe–O layer.

0022-4596/99 $30.00

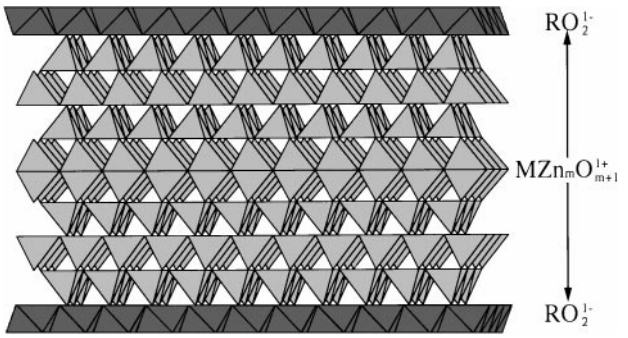

FIG. 1. Schematic drawing of the basic structure of $RMO_3(ZnO)_m$. Two neighboring R–O layers are interleaved by $m + 1$ ($= 7$) M/Zn–O layers.

2. EXPERIMENTAL

A solid-state reaction method was used for the sample preparation. Prior to mixing, Fe_2O_3 and ZnO powders were heated at 1273 K for 1 day. A mixture of Fe_2O_3 and ZnO in a determined mole ratio was heated in a Pt-sealed tube at 1523 K for 7 days and then rapidly cooled to room temperature. In the present work, the Fe_2O_3 : ZnO mole ratio in the raw material was 1:13. The X-ray diffraction pattern reported in the previous paper was indexed by considering the compound $Fe_2O_3(ZnO)_{13}$ (2, 3). It is the character of the present homologous compound series that with the increase of the ZnO mole percentage, i.e., the increase of m in the chemical formula, the solid-state reaction is very slow. The synthesized material may contain compounds with different m numbers. In fact, we selected $Fe_2O_3(ZnO)_{15}$ from the above synthesized material to be observed by transmission electron microscopy for the following reasons. First, no compounds with m larger than 8 have been synthesized (14, 15), in the $Fe_2O_3(ZnO)_m$ system and according to our previous experience, the modulated structures appear only in compounds with large m ($m > 6$) (10, 12, 13). Second, the crystallography of compounds with large odd m numbers is much better than those with large even m numbers (2, 3).

For electron microscope observations, the samples were crushed in an agate mortar and dispersed onto a holey carbon grid by using a CCl_4 solution. Selected-area electron diffraction patterns and corresponding lattice images were observed by using a high-resolution electron microscope (JEM-2000EX), operated at 200 kV. The Cs value of the electron microscope is 0.7 mm and its resolution is 0.20 nm.

3. RESULTS AND DISCUSSION

The electron diffraction pattern of $Fe_2O_3(ZnO)_{15}$ and its corresponding schematic drawing are shown in Figs. 2a and 2b. Both the main and satellite spots are observed, implying the formation of a modulated structure. As illustrated in the previous paper, because of the appearance of the satellite spots, this diffraction pattern cannot be indexed by considering the hexagonal unit cell as suggested by X-ray diffraction analysis. Instead, it can be indexed by considering a monoclinic unit cell where the main and satellite spots are indexed as $h\mathbf{a}^* + k\mathbf{b}^* + l\mathbf{c}^* + m\mathbf{q}$. The parameters for the monoclinic unit cell are $a = 0.57$ nm, $b = 0.33$ nm, $c = 4.5$ nm, and $\beta = 92^\circ$, where $\mathbf{b}$ was taken as the unique axis. The modulation wave vector $\mathbf{q} = \mathbf{b}^*/s + \mathbf{c}^*/2$ ($s = 34.8$) contains not only the irrational parts $\mathbf{q}_i = \mathbf{b}^*/s$ but also the rational parts $\mathbf{q}_r = \mathbf{c}^*/2$. Figure 2b shows schematically the relation between the reciprocal lattice base vectors $\mathbf{a}^*$, $\mathbf{b}^*$, and $\mathbf{c}^*$ and the modulation wave vectors $\mathbf{q}_i$ and $\mathbf{q}_r$. In the monoclinic crystal system, the diffraction pattern of Fig. 2a corresponds to the $\mathbf{b}^*$–$\mathbf{c}^*$ reciprocal lattice section. This diffraction pattern is very important in the analysis of modulated structure because it shows clearly the relative layout of the main and satellite spots and also because the ordering of ions can be imaged directly in the corresponding high-resolution image. Based on the results of our previous analysis, the possible space groups for the basic structure are $C2$, Cm, and $C2/m$. These possible three-dimensional space groups for the basic structure together with the modulation wave vector $\mathbf{q} = \mathbf{b}^*/s + \mathbf{c}^*/2$ lead to the possible superspace groups C_1^{C2}, $C_{\bar{1}}^{Cm}$, and $C_{1\bar{1}}^{C2/m}$ for the modulated structure. The expressions of these superspace groups are the same as those suggested by Yamamoto (16, 17) and correspond to B_1^{B2}, $B_{\bar{1}}^{Bm}$, and $B_{1\bar{1}}^{B2/m}$ suggested by Wolff (18–20). To express the extinction condition of the satellite spots in these superspace groups, a set of base vectors which make the modulation wave vectors contain no rational part is usually taken. This purpose can be realized by introducing the reciprocal lattice base vectors $\mathbf{a}_s^* = \mathbf{a}^*$, $\mathbf{b}_s^* = \mathbf{b}^*$, and $\mathbf{c}_s^* = \mathbf{c}^*/2$. The main and satellite spots can then be indexed as $H\mathbf{a}_s^* + K\mathbf{b}_s^* + L\mathbf{c}_s^* + m\mathbf{q}_i$. Expressed by H, K, L, and m, the common and the only extinction condition for the satellite spots of the above possible superspace groups is $HKLm: L + m = 2n$. The indices in Figs. 2a and 2b correspond to H, K, L, and m. The extinction condition of the satellite spots in Fig. 2a is $0KLm: L + m = 2n$, which is obviously the special case of $HKLm: L + m = 2n$.

Figure 3 shows the high-resolution image corresponding to the diffraction pattern of Fig. 2a. From the contrast similarity to that of $InFeO_3(ZnO)_m$ (10, 11), the Fe–O and Fe/Zn–O layers are indicated in the figure. The zigzag or wavy contrast within the Fe/Zn–O layers corresponds to the modulated structure. The 11.5-nm average periodicity along the $\mathbf{b}$ direction is in agreement with sb, which corresponds to the component of modulation wave vector $\mathbf{q}$ along the $\mathbf{b}^*$ direction. The angle of the zigzag contrast with the Fe–O layer is about 40°. These features in terms of the angle and the periodicity of the zigzag contrast are very similar to those of $InFeO_3(ZnO)_m$ reported earlier. From the results of $InFeO_3(ZnO)_m$ (11), it is reasonable to consider that the present modulated structure is caused by the ordering of Fe

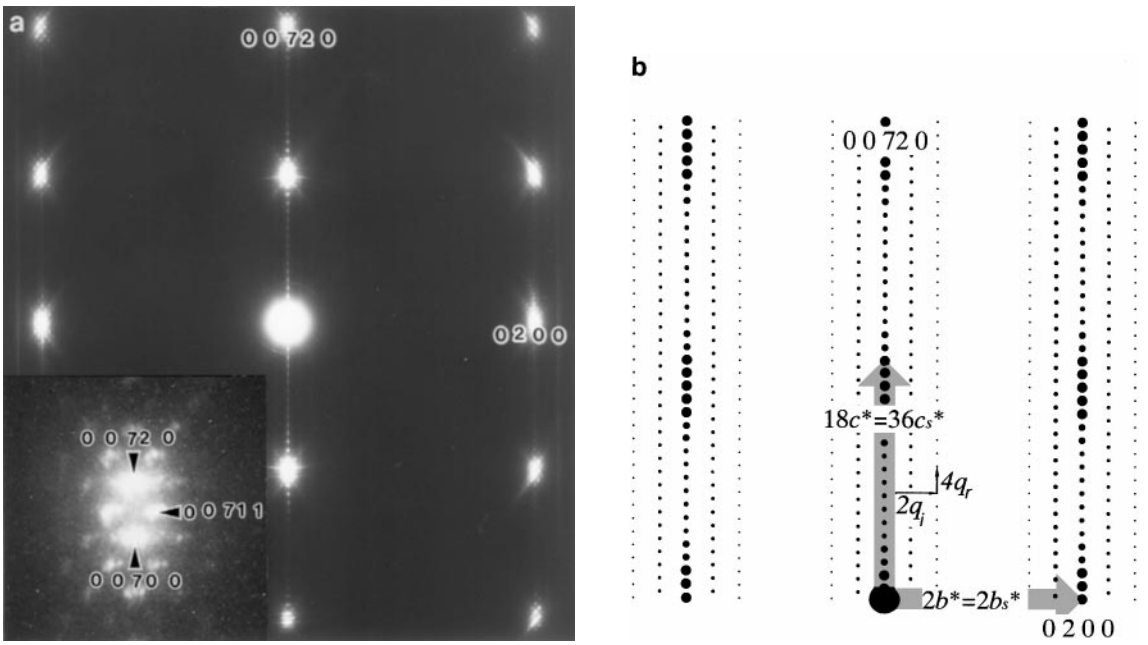

FIG. 2. (a) Electron diffraction pattern of $Fe_2O_3(ZnO)_{15}$ showing the **b***–**c*** reciprocal lattice section. The inset shows the enlarged area around (0,0,72,0). (b) Schematic drawing of (a) showing the relation between the monoclinic reciprocal lattice base vector and the modulation wave vector.

ions in the Fe/Zn–O layers. There are two special features in Fig. 3 which have not been observed in the modulated structures reported previously: the periodic contrast variation of the Fe–O layer and the *sb*/2 relative shift of two neighboring zigzag-shaped contrasts along the *b* axis direction. The periodicity of the Fe–O layer contrast variation is about one-third that of the zigzag contrast in the Fe/Zn–O layers. Since there is only one element, Fe, occupying the octahedral site in the Fe–O layer, this modulated structure must be caused by the displacement of Fe ions. In the electron diffraction pattern, the modulated structure of Fe–O layers corresponds to the diffuse scattering lines

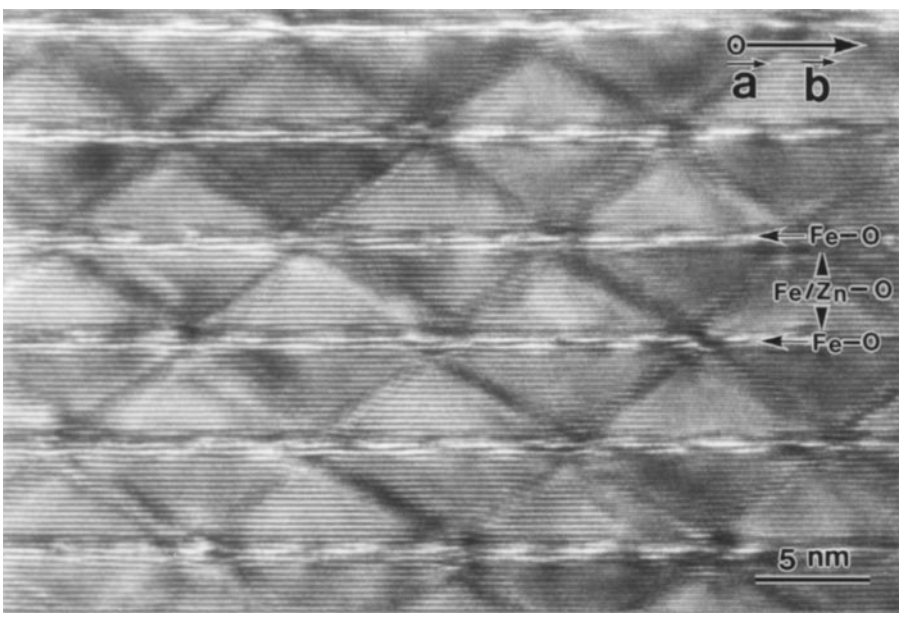

FIG. 3. High-resolution image of $Fe_2O_3(ZnO)_{15}$. The corresponding electron diffraction pattern is shown in Fig. 2a.

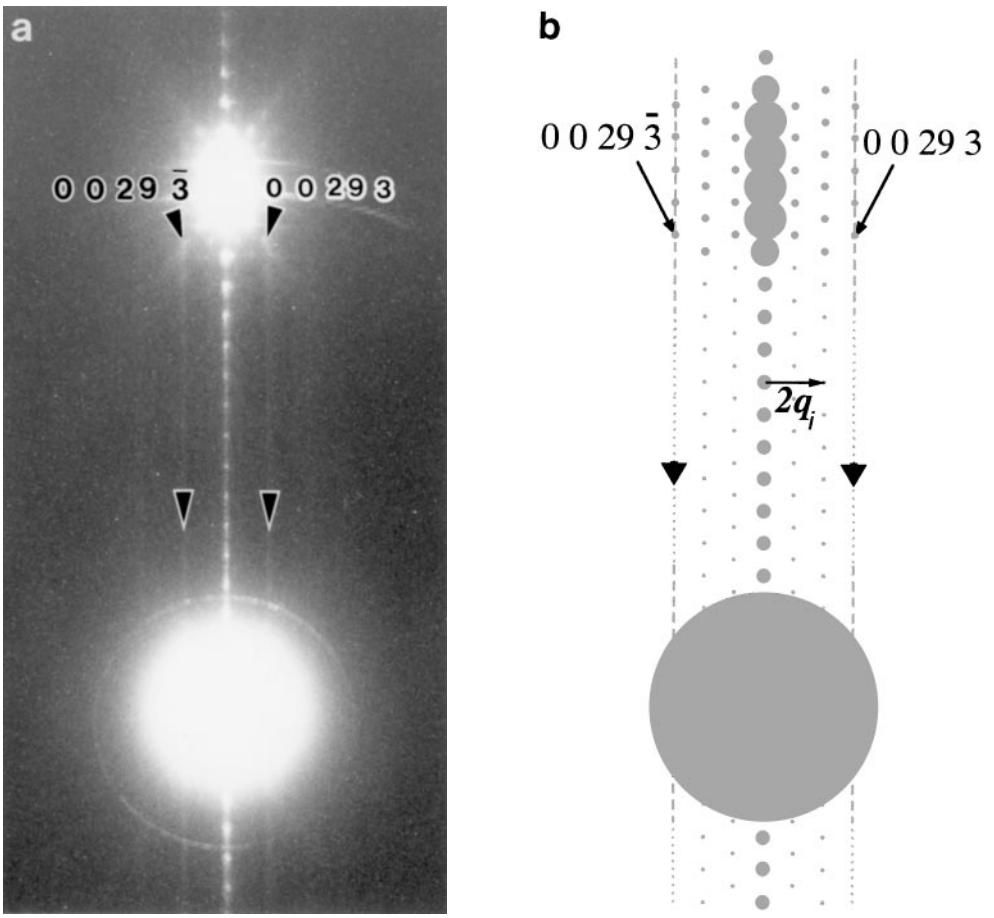

FIG. 4. (a) Electron diffraction pattern of $Fe_2O_3(ZnO)_{15}$ showing the **b***–**c*** reciprocal lattice section. The diffuse scattering lines indicated by arrows correspond to the modulated structures of the Fe–O layers. (b) Schematic drawing of (a) showing the relative layout of the satellite spots and the diffuse scattering lines.

parallel to the c^* axis which is indicated by arrows in Fig. 4a. Figure 4b is a schematic drawing of Fig. 4a, showing the relative layout of the diffuse scattering line with the satellite spots. The distance of this line from the **c*** axis is three times that of $\mathbf{q}_i = \mathbf{b}^*/s$, which is in agreement with the high-resolution image observation. With respect to the shift of the zigzag-shaped contrast, if one considers the zigzag contrast as a wave, the above relative shift can also be understood as a phase difference of π between neighboring zigzag-shaped contrasts. In this sense, the modulated structure in Fig. 3 can be called an antiphase modulated structure and those without shift in-phase modulated structures.

It should be pointed out that areas with an in-phase modulated structure can also be observed in $Fe_2O_3(ZnO)_{15}$. The image of Fig. 5 shows the coexistence of antiphase and in-phase modulated structures. The upper part is the in-phase modulated structure and the lower part is the antiphase modulated structure. It is worth mentioning that in $Fe_2O_3(ZnO)_{15}$ the probability of observing the in-phase modulated structure is much lower than that of observing the antiphase modulated structure.

Figure 6 shows the modulated structure model of $Fe_2O_3(ZnO)_{15}$ projected along the [100] direction. The Fe–O and Fe/Zn–O layers are represented by different lines. There are 16 Fe/Zn–O layers between 2 Fe–O layers. The atomic location on these lines is not depicted because their separation, which is estimated to be 0.17 nm, is narrower than the 0.20-nm resolution limit of the present electron microscope. The modulation of the Fe–O layer is represented by the curving of the corresponding lines. The thick area in the Fe/Zn–O lines represents the place where Fe is enriched. These areas are arranged in a zigzag shape in accordance with the high-resolution image of Fig. 3. Across the Fe–O layer, this zigzag-shape shifts along the **b** direction by $sb/2$. In the following, we will illustrate that this shift corresponds to the rational part of the modulation wave vector. From the superspace group point of view, the probability of Fe occupaying an Fe/Zn site can be described by

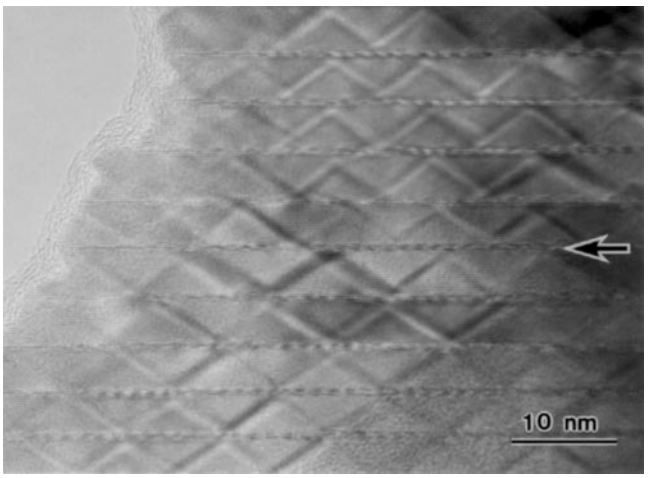

FIG. 5. An image of $Fe_2O_3(ZnO)_{15}$ showing the coexistence of antiphase (the lower part) and in-phase (upper part) modulated structures.

a periodic function $P[2\pi(\mathbf{q}\cdot\mathbf{r} + u)]$, where $\mathbf{q}$ is the modulation wave vector, $\mathbf{r}$ is the position vector of this site referred to the origin of a selected unit cell, and u is a phase factor (16, 20). Using the monoclinic unit cell base vector, one can express $\mathbf{r}$ as $\mathbf{r} = n_1\mathbf{a} + n_2\mathbf{b} + n_3\mathbf{c} + x\mathbf{a} + y\mathbf{b} + z\mathbf{c}$, where n_1, n_2, and n_3 are the unit cell numbers from the origin along the **a**, **b**, and **c** directions, respectively, and x, y, and z are the coordinates of this site within the unit cell. Replacing $\mathbf{r}$ with $n_1\mathbf{a} + n_2\mathbf{b} + n_3\mathbf{c} + x\mathbf{a} + y\mathbf{b} + z\mathbf{c}$ and $\mathbf{q}$ with $\mathbf{b}^*/s + \mathbf{c}^*/2$, $\mathbf{q}\cdot\mathbf{r}$ becomes $(n_2 + y)/s + (n_3 + z)/2$. Then, the above distribution function becomes $P\{2\pi[(n_2 + y)/s] + \pi(n_3 + z) + 2\pi u\}$. For a special Fe/Zn–O layer the n_3 and z are determined, and the above function becomes the distribution function of Fe and Zn along the **b** direction in that layer, which has a periodicity of sb. For example, the functions for the I-1 and II-1 Fe/Zn–O layers in Fig. 6 are $P\{2\pi[(n_2 + y)/s + z/2 + u]\}$ and $P\{2\pi[(n_2 + y)/s + z/2 + u] + \pi\}$, respectively. They are the same except for a phase difference of π, which means that the distribution of Fe and Zn atoms in the I-1 and II-1 layers is the same except for a shift of $sb/2$. The same discussion applies to other corresponding layers, e.g., the I-2 and II-2 layers and the I-3 and II-3 layers. As a result, the entire zigzag shape in the lower Fe/Zn–O layer block shifts along the **b** direction by $sb/2$ relative to the upper one.

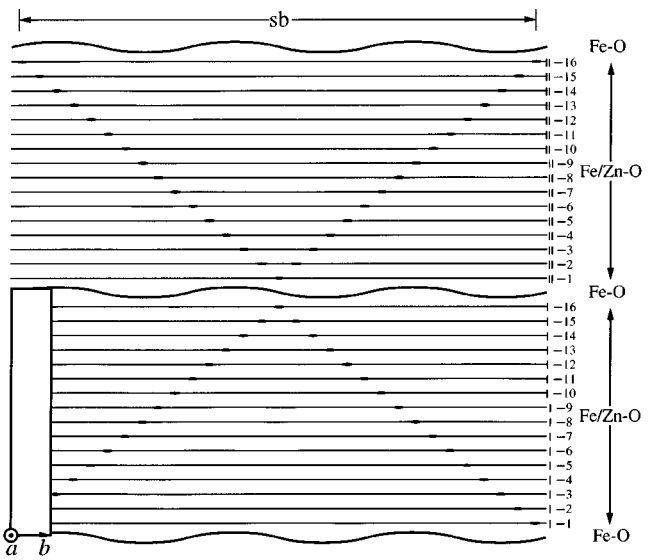

FIG. 6. A modulated structure model of $Fe_2O_3(ZnO)_{15}$. The thick area in the Fe/Zn–O layer represents atomic sites where Fe is enriched, and the curving of the Fe–O layer represents the modulated structure of the Fe–O layer.

Since the R sites are occupied by different ions in $InFeO_3(ZnO)_m$ and $Fe_2O_3(ZnO)_m$, comparison of the modulated structures of $InFeO_3(ZnO)_m$ and $Fe_2O_3(ZnO)_m$ would be meaningful for the understanding of the role of R in the formation of the modulated structure. The modulated structure of $InFeO_3(ZnO)_m$ and $Fe_2O_3(ZnO)_m$ agree with each other in terms of the periodicity and the angles of the zigzag contrasts with the In–O(Fe–O) layers. However, in $Fe_2O_3(ZnO)_m$, the neighboring zigzag contrasts shift mutually by half of their periodicity whereas in $InFeO_3(ZnO)_m$, this shift is zero. In addition to the above difference of the modulated structures in M/Zn–O layers, the substitution of In by Fe in the R–O layer also causes the variation of the R–O layer itself: the In–O layer in $InFeO_3(ZnO)_m$ is not subjected to modulation whereas the Fe–O layer in $Fe_2O_3(ZnO)_m$ is subjected to modulation.

We consider the difference of the ionic radii of In and Fe to be the reason for the formation of different modulated structures in $InFeO_3(ZnO)_m$ (R = In) and $Fe_2O_3(ZnO)_m$ (R = Fe). The In (Fe) ions occupy the octahedral sites of the close-packed oxygen ions in the In–O (Fe–O) layers. In the present homologous compound series, the typical distance from the center of such an octahedron to the nearest oxygen ion is estimated to be 0.23 nm. The necessary distance for In and Fe ions to occupy this site is estimated to be 0.22 and 0.20 nm from the ionic radii, respectively (21). Since the In ions fit the octahedral site better than Fe, it is reasonable to consider that the In–O layer is more stable than the Fe–O layer. On the other hand, it is reasonable to consider that the ordering of Fe causes a structural stress field in the Fe/Zn–O layer block. Because of the different character of the Fe–O and In–O layers, the mutual interaction of the stress fields across the Fe–O/In–O layers or the interaction of the stress field with the Fe–O/In–O layers will be different, which, we believe, are the reasons for the formation of different modulated structures in $Fe_2O_3(ZnO)_m$ and $InFeO_3(ZnO)_m$.

4. CONCLUSION

The modulated structure of $Fe_2O_3(ZnO)_{15}$ has been studied by high-resolution transmission electron microscopy and compared with those of $InFeO_3(ZnO)_m$ reported

in an earlier paper. The main and satellite spots are indexed as $h\mathbf{a}^* + k\mathbf{b}^* + l\mathbf{c}^* + m\mathbf{q}$ by considering a monoclinic unit cell and a modulation wave vector $\mathbf{q}$. $\mathbf{q} = \mathbf{b}^*/s + \mathbf{c}^*/2$ includes both the irrational part $\mathbf{b}^*/s$ and the rational part $\mathbf{c}^*/2$. The possible space groups are assigned as $C2$, Cm, and $C2/m$ for the basic structure and the possible four-dimensional superspace groups are assigned as C_1^{C2}, $C_{\bar{1}}^{Cm}$, and $C_{1\bar{1}}^{C2/m}$ for the modulated structure. In the high-resolution image, the zigzag-shaped modulated structure contrasts within the Fe/Zn–O layers shift each other by half of the periodicity. Further, modulation of the Fe–O layer, which is not found in other systems, is observed in the present compound. By comparing the results of $InFeO_3(ZnO)_m$ and $Fe_2O_3(ZnO)_m$, it is recognized that R ions affect the symmetry of the modulated structure of $RMO_3(ZnO)_m$.

REFERENCES

1. H. Kasper, *Z. Anorg. Allg. Chem.* **349,** 113 (1967).
2. N. Kimizuka, T. Mohri, and M. Nakamura, *J. Solid State Chem.* **81,** 70 (1989).
3. M. Nakamura, N. Kimizuka, and T. Mohri, *J. Solid State Chem.* **86,** 16 (1990).
4. M. Nakamura, N. Kimizuka, and T. Mohri, *J. Solid State Chem.* **93,** 298 (1991).
5. M. Nakamura, N. Kimizuka, T. Mohri, and M. Isobe, *J. Solid State Chem.* **105,** 535 (1993).
6. H. Ohta, W. Seo, and K. Koumoto, *J. Am. Ceram. Soc.* **79,** 2193 (1996).
7. M. Isobe, N. Kimizuka, M. Nakamura, and T. Mohri, *Acta Crystallogr., Sect. C* **50,** 332 (1994).
8. N. Kimizuka, M. Isobe, and M. Nakamura, *J. Solid State Chem.* **116,** 170 (1995).
9. P.J. Cannard and R.J.D. Tilley, *J. Solid State Chem.* **73,** 418 (1988).
10. N. Uchida, Y. Bando, M. Nakamura, and N. Kimizuka, *J. Electron Microsc.* **43,** 146 (1994).
11. Y. Bando, Y. Kitami, K. Kurashima, T. Tomita, T. Honda, and Y. Ishida, *Microbeam Anal.* **3,** 279 (1994).
12. C. Li, Y. Bando, M. Nakamura, and N. Kimizuka, *J. Electron Microsc.* **46,** 119 (1997).
13. C. Li, Y. Bando, M. Nakamura, and N. Kimizuka, *J. Solid State Chem* (submitted).
14. N. Kimizuka, M. Isobe, M. Nakamura, and T. Mohri, *J. Solid State Chem.* **103,** 394 (1993).
15. M. Nakamura, N. Kimizuka, T. Mohri, and M. Isobe, *J. Alloys Comp.* **192,** 105 (1993).
16. A. Yamamoto, T. Janssen, A. Janner, and P. M. D. E. Wolff, *Acta Crystallogr., Sect. A* **41,** 528 (1985).
17. A. Yamamoto, *Acta Crystallogr., Sect. A* **52,** 509 (1996).
18. P. M. De. Wolff, T. Janssen, and A. Janner, *Acta Crystallogr., Sect. A* **37,** 625 (1981).
19. P. M. De. Wolff, *Acta Crystallogr., Sect. A* **33,** 493 (1977).
20. A. Janner, T. Janssen, and P. M. De. Wolff, *Acta Crystallogr., Sect. A* **39,** 658 (1983).
21. R.D. Shannon, *Acta Crystallogr., Sect. A* **32,** 751 (1976).